Automated 3D Quantitative Analysis of Digital Microstructure Images of Materials using Stereology

P.S.Hiremath
Department of Computer Science
Gulbarga University,
Gulbarga-585 104. India

Anita Sadashivappa
Department of Computer Science and Engineering
P.D.A. College of Engineering,
Gulbarga –585 102.India

ABSTRACT
In material testing process, the assessment of 3D geometry from 2D microstructure images of materials using stereological methods seems to gain more importance. An exclusive field by name Stereology (collection of stereological methods) has evolved to address the quantitative analysis of materials. The stereology by manual practice is tiresome, time consuming and often produce biased results due to manual physiological limits. There is a definite need for automation of stereological procedures that can make greater impact on quality of quantitative analytical results. In this paper, an automated method to derive quantitative description of 3D geometry based on data obtained by quantitative image analysis of 2D digital microstructure images is proposed. The proposed method makes use of stereological parameters and digital image processing techniques for estimation of many stereological parameters (proposed by American Standard for Materials - ASM). The results obtained by proposed method correlate with the results obtained by manual methods satisfactorily. Further, it saves considerable amount of effort, time and cost in material testing process. Since the basic frame-work of the proposed method considers many quantifiable parameters which are otherwise difficult in manual process, it has practical significance in material testing laboratories.

General Terms
Material science, phase, ASM(American Standard for materials).

Keywords
Stereology, Otsu's segmentation, cast iron, microstructure.

1. INTRODUCTION
Many applied disciplines, namely, material science, biology, medicine, mineralogy and geology require understanding of qualitative and quantitative properties of materials. Also, manufacturing experts need to know material behavior and variation during processing and in use. The quantitative information of microstructure is of practical importance in material science and engineering along with other necessary information, e.g. chemical and physical data, and geometric properties of microstructures, to characterize the state of the given material, to interpret many of its physical behaviors and functions, and to perform quality control of the microstructure processes [1].

There are many measurements that can be made including size, shape, position, etc. of the structures found in microstructure images. Every material has 3D structure and most of the measured values are not directly related to the 3D structure that is present and represented in the image. Also, the measurements may not be meaningful unless the measurements are not based on principles of Stereology [2, 4]. In [4, 5, 7, 8, 9], the relations and procedures used for deriving quantitative information from a 2D microstructure image are described. In [10], the methods for statistical analysis of microstructures are discussed. A systematic analysis which can reduce errors in results of quantitative analysis is presented in [11]. In [12], authors have proposed a method for quantification of volume fraction of ferrite and graphite phases in digital microstructure images of low-carbon steel. In [13], various methods for deriving quantitative information of material structures from digital images have been described. In [14], two microstructure analysis methods, namely, stereology and direct assessment of 3D microstructures are compared and it is observed that although direct 3D assessments of microstructures has more advantages, the importance of stereological methods cannot be ignored. The literature survey indicates that for the measurements, namely, point intersections, line length, area, etc. the manual methods are used predominantly. Few attempts of automating the manual based stereological methods have been reported [4,5,6,8,9,11,13,17]. A complete automated stereology system which is accurate and affordable to medium scale test laboratories is still a due.

Majority of the stereology based works reported in the literature are aimed towards applications in biological science. As the stereology is an interdisciplinary field and the methods based on stereology are generic in nature, these methods are applicable to material science applications also. The main aim of this paper is to present a novel automated stereology system for digital microstructure image analysis in material science applications. The stereology relations and manual methods practiced in stereology are described in the Section 2. In the Section 3, the proposed method is presented. The experimental results are given in the Section 4. The Section 5 contains the conclusion.

2. STEREOLOGY
Stereology (from Greek, stereos = solid) was originally defined as "the spatial interpretation of sections". It is an interdisciplinary field that is largely concerned with the three-dimensional interpretation of planar sections of materials or tissues. International Society for Stereology has tried to standardize the terminology as well as the nomenclature [1]. It provides practical techniques for extracting quantitative information about a three-dimensional material from measurements made on two-dimensional planar sections of the material. Stereology utilizes random systematic sampling to provide unbiased and quantitative data [2, 4]. It is an important and efficient tool in many applications of microscopy, such as petrography, materials science, and biosciences.

Stereological relationships provide a set of equations that can relate some of the measurements on the 2D images to important parameters of the actual 3D structure. The classical stereology has proposed manual methods for evaluating the volume, surface, length, curvature and number of spatial structures from their sections or projections. All the stereological principles are characterized by the fact that the random interaction between the structural object and a geometric reference system (a grid, a plane, or a sweeping line) leads to an observable result which occurs with a predictable probability.

2.1 Stereological relations

The stereology as applied to practical problems uses a set of 'global parameters' [14]. Each global parameter provides an unbiased estimate of a specific geometric characteristic of the entire microstructure present in an image. Each global parameter is a simple (normalized) sum and, irrespective of the mixture of shapes, sizes and mutual arrangement of grains, particles, pores, cells, etc., can be expressed by a simple value without reference to other parameters. The most important advantage is that these parameters define those quantities which can be directly related to the properties and functions of a material by physical reasoning. The two most useful global parameters are volume fraction and interface densities.

The Table 1 and Table 2 show some of the important global parameters for single-component and two-component materials that are applied on 2D sections of material objects, whose results can be used to infer 3D geometric characteristics of the material [14].

2.2 Manual based counting procedures in practice

The lines or points in the grids are probes that interact with the structure revealed by the microscope section image. The grids are used to overlay onto images for quantification of microstructures. The Fig.1 and Fig.2 show counting procedures for determining global parameters [14]. Counting the hits the grids make with particular structures generates the raw data for analysis. There are several advantages to using the computer to generate grids to overlay onto the image. In contrast to the manual method of placing transparent grids onto photographic prints, the computer method avoids the need for photography and printing.

Generally, the global parameters listed in the Table 1 and Table 2 are determined manually and semi-automated methods, but the digital image processing techniques offer better alternative methods, which minimize human efforts, provide accurate results, save cost and considerable amount of time.

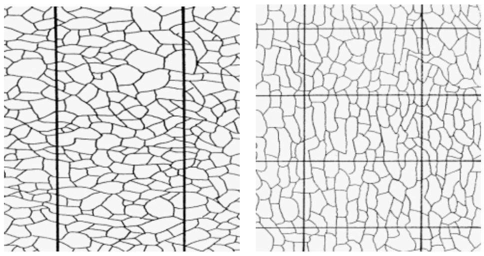

(a) (b)

Fig.1: Counting procedures for determining global stereological parameters in single-component microstructures: a) isotropic grain structure, counting of number of intersection points of boundary with test line, P_L; b) oriented grain structure, counting of intersection points with test lines oriented in and perpendicular to orientation directions, $P_{L(or)}$ and $P_{L(\mathrm{perp})}$ [14].

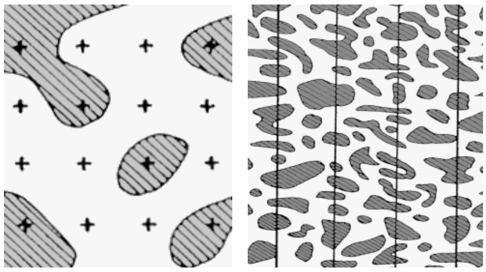

(a) (b)

Fig.2: Counting procedures for determining global stereological parameters in two- and multi-component microstructures: a) counting hit points with a point grid in two fields for determining the volume fraction; b) counting the number of intersection points of test lines with $\alpha\beta$ -interface, $P_{L(\alpha\beta)}$ [14].

3. PROPOSED METHODOLOGY

The general framework of the proposed methodology is shown in Fig. 3.

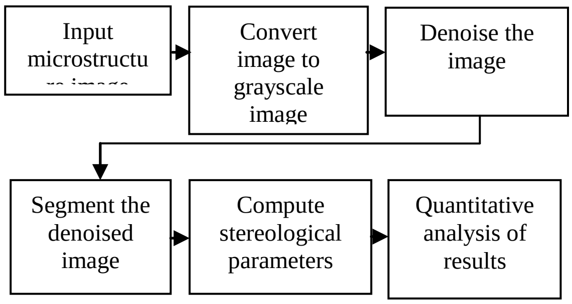

Fig.3. General framework of the proposed methodology

3.1 Materials used

In the proposed work, one-component and two-component images of materials are considered for experimentation. For one-component material, ferrous material images and for two-component material, low-carbon cast iron microstructure images of various compositions are employed. The microstructure images have been drawn from the microstructure library [15]. For experimentation, we have used 104 microstructure images where 8 images are of one-component (Ferrite) microstructure and 96 images are of two-component (Ferrite and Graphite) microstructure. Some of the sample microstructure images used in experimentation are presented in the Fig.4.

Table 1. Important global parameters for single – component materials

Global 3D parameters and stereological relationship	Examples of application	Related 2D quantity on cross section
Boundary density, $S_v = 2P_L$	Grain boundary area, Cell boundary area.	Number of intersection points of boundary with test line, P_L.
Mean linear size, $\overline{L} = I/P_L = 2/S_V$	Mean linear cell size, Mean linear grain size.	Number of intersection points of boundary with test line, P_L.
Degree of orientation, $F_{(or)} = 2P_{L(or)}/(P_{L(or)} + P_{L(perp)})$ $= S_{v(or)}/S_{v(tot)}$	Oriented fraction, $S_{v(or)}$, total (isotropic and oriented) interfaces, $S_{v(tot)}$, in drawn or extruded materials, tree cells.	Number of intersection points with test lines oriented in and perpendicular to orientation directions, $P_{L(or)}$ and $P_{L(perp)}$.

Table 2. Important global parameters for two – component materials

Global 3D parameters and stereological relationship	Examples of application	Related 2D quantity on cross section
Volume fraction, $V_V = A_A = L_L = P_P$	Fractions of components, Materials density	Area fraction, A_A. Line fraction, L_L. Point fraction, P_P
Interface density $S_v = 2P_L$	Interface area between phases or components, pore–solid interface	Number of intersection points between interface and test line, P_L
Mean linear size, $\overline{L} = P_P/P_L = 2V_V/S_V$	Mean particle size, Mean cell size, Mean pore size.	Point fraction, PP, number of intersection points between interface and test line, P_L
Mean linear distance $\overline{D} = (1-P_P)/P_L = 2(1-V_V)/S_V$	Mean linear distance (mean free path) between particles, cells, pores, etc.	P_P and P_L See mean linear size
Contiguity, $C^{\alpha\alpha} = P_{L(\alpha\alpha)}/(P_{L(\alpha\beta)} + P_{L(\alpha\alpha)})$ $= S_{V(\alpha\alpha)}/S_{v(tot)}$	Fraction of spatial area shared with other grains of component α connectiveness	Number of intersection points of test lines with grain *(αα)* boundaries, $P_{L\ (\alpha\alpha)}$, and with *(αβ)* interfaces, $P_{L\ (\alpha\beta)}$.
Neighborhood, $C^{\alpha\beta} = P_{L(\alpha\beta)}/(P_{L(\alpha\beta)} + P_{L(\alpha\alpha)})$ $= S_{V(\alpha\beta)}/S_{v(tot)}$	Fraction of interface shared by components *α* and *β* connectivity of different components	$P_{L\ (\alpha\beta)}$ and $P_{L\ (\alpha\alpha)}$, See contiguity.
Degree of orientation, $F_{(or)} = 2P_{L(or)}/(P_{L(or)} + P_{L(perp)})$ $= S_{V(or)}/S_{v(tot)}$	As for single component materials, for directionally cast structure, oriented structures in plants or tissues.	Number of intersection points with test lines oriented in and perpendicular to orientation directions, $P_{L\ (or)}$ and $P_{L\ (perp)}$.

Table 3. Values of global stereological parameters derived by manual method, using the horizontal grid size with 5 probes each of size 300 µm on sample microstructure images each of size 470x365 µm (571x480 pixels) shown in Fig.4. (Scale factor: 1 pixel=0.625µm)

The proposed method comprises the following steps: Conversion of input image to grayscale image, denoising the image, image segmentation, computation of stereological parameters, which are described below.

3.2 De-noising and Image Segmentation

Generally, microstructure images suffer from impulse noise. and in the proposed methods, the microstructure images are pre-processed by applying 'selective median switching filter' [16] for suppressing the impulse noise present in microstructure images. Then the filtered image is segmented using Otsu's segmentation method [8] for segmentation of various regions present in filtered microstructure images. Then various global stereological parameters are determined.

3.3 Computation of Stereological Parameters

The global stereological parameters of 3D images using 2D section image analysis, based on digital image processing techniques, are compared as described below.

Determining volume fraction

The one-component and two-component (or two phase- *α* and *β*) microstructure images are shown in Fig. 5(a) and 5(b), respectively. The image, 5(a)(i) is filtered and segmented (Fig.5(a)(ii)). The filtered and segmented image is subjected to edge enhancement using morphological operations, namely, dilation and skeletonization (Fig. 5(a)(iii)). The 5(b)(i) image is a two-component microstructure image. It is filtered and segmented and obtained binary image, 5(b)(iii). It contains two distinct regions, namely, the white region (Pearlite/Graphite – α

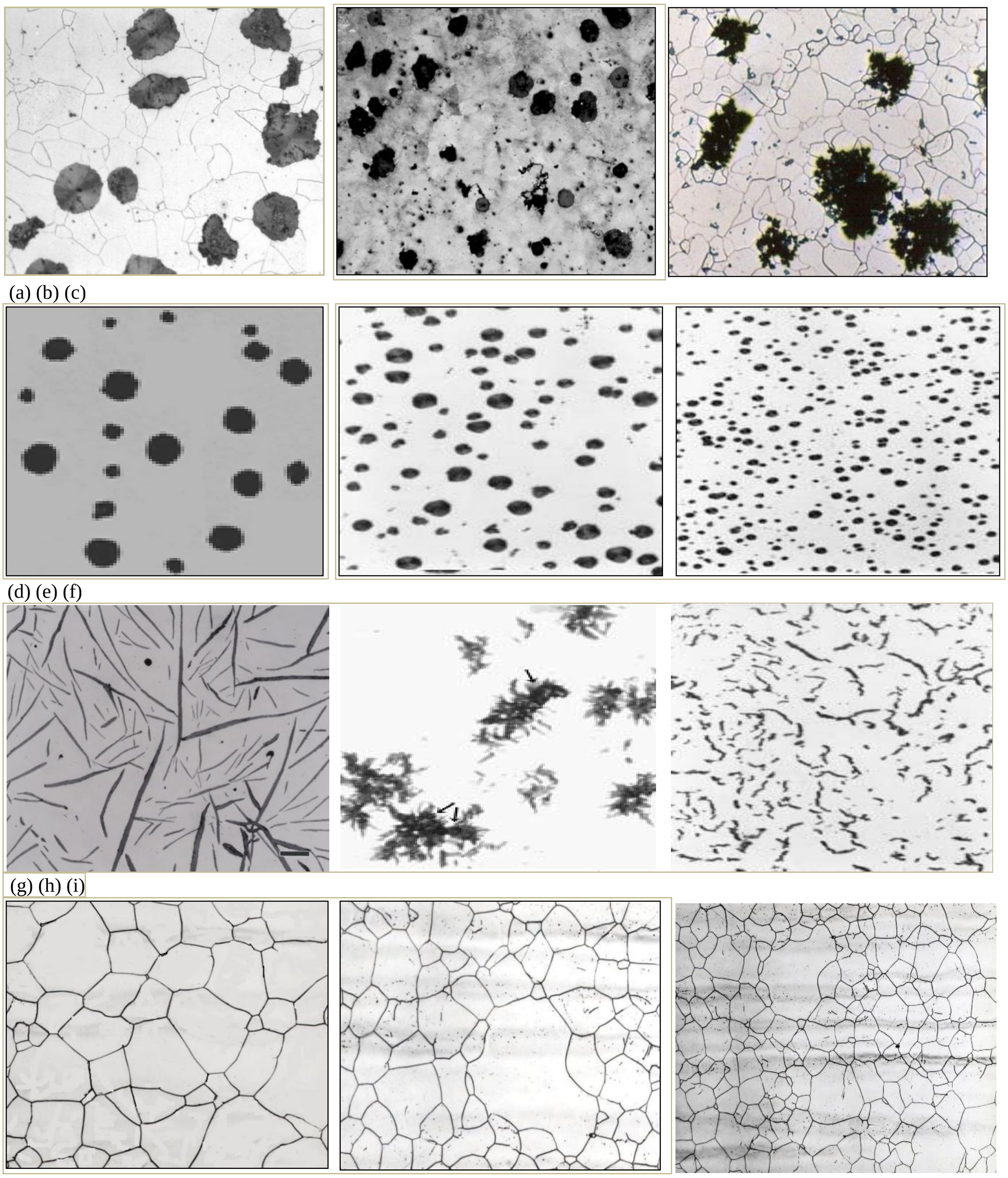

(a) (b) (c)
(d) (e) (f)
(g) (h) (i)
(j) (k) (l)

Fig.4: Sample microstructure images of cast iron: (a)–(i) Two-component and (j)-(l) One-component material microstructure images. Wt. percentage of C in microstructure 4(a)-5%, 4(b)-2.9%, 4(c)-4.2%,4(d)-2.9%,4(e)-3.5%.

phase) and black background (Ferrite- β phase). For filtering, SMSF method [16] and for segmentation, Otsu's segmentation method [8] are employed. The pixels belonging to the regions are counted (total area of regions) and volume fraction is determined using the relation;

$$V_v = \sum_R Area\_of\_segments \quad (1)$$

where R is the regions in the segmented image.

Determining P_L The P_L, is basis value in determining many other stereological parameters. For determining the P_L value, the boundary image from the segmented image is generated. In the boundary image, the boundary of regions has thickness of single pixel (Fig. 5(c)). The count of these boundary pixels gives the P_L value [4]. In computation of P_L value, the following relation is used.

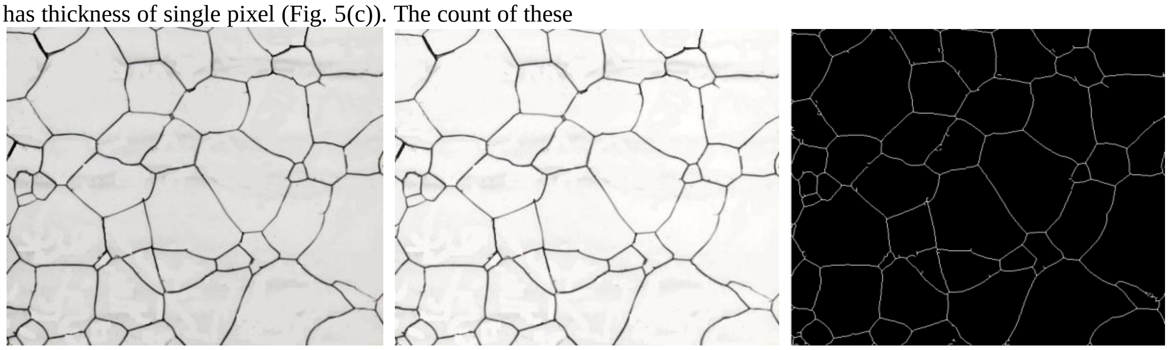

(i) (ii) (iii)

Fig. 5(a): Pre-processing of one-component material microstructure image. (i) Original microstructure image, (ii) Filtered image and segmentation, (iii) Grains boundary Image.

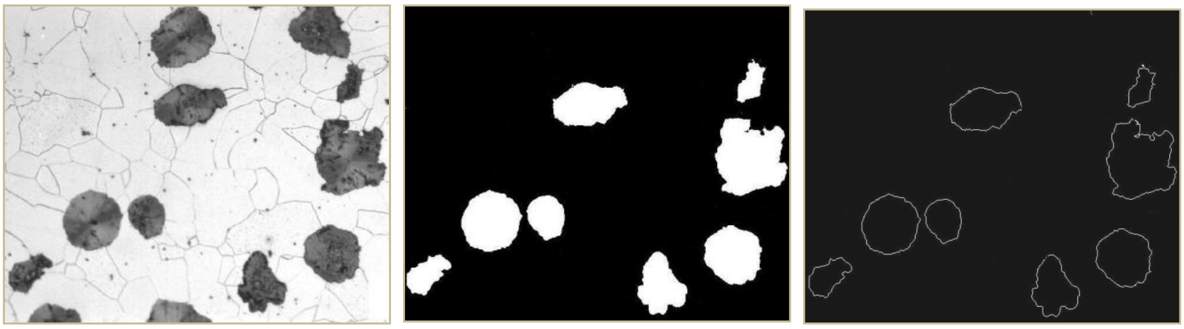

(i) (ii) (iii)

Fig. 5(b): Pre-processing of two-component material microstructure image. (i) Original microstructure image, (ii) Filtered and Segmented image, (iii) Boundary Image

$$P_L = \sum_R Pixels\_on\_Perim\_of\_regions \qquad (2)$$

where R is the regions in the segmented image.

Using the value of P_L, most of the stereological parameters are determined by substitution in the relations shown in the Table 1 and Table 2.

Counting total number of grains

For counting total number of grains in the microstructure image, the segmented image regions are first labeled. The maximum label value determined in the labeled image is taken as the total number of grains in the image.

Computing grain size

For computing the size of each grain, the segmented and labeled image is used. The area of each labeled region is computed. Average of the computed area of grains gives the average size of grains in the sample microstructure and the maximum area of the grain is taken as maximum size of grain in the image.

3.4 Proposed Algorithms

The proposed method is presented in the following algorithms, the Algorithm 1 being used for one-component microstructure image while the Algorithm 2 being used for two-component microstructure image.

Algorithm 1: For processing one-component microstructure images

1. Input RGB microstructure image, I_{RGB}
2. Convert I_{RGB} image to grayscale image, I_{Gray}.
3. De-noise the image I_{Gray} using SMSF method and obtain filtered image, $I_{Filt.}$.
4. Segment the I_{Filt} image using Otsu's segmentation method and obtain segmented binary image, I_{Seg}.
5. Enhance the grain boundaries by morphological operations, namely, dilation and skeletonization to generate grains boundary image, I_{Perim} of I_{Seg} image.
6. Compute P_L using Eq.(2).
7. Compute boundary (interface) density using relation; $S_v = 2P_L$.
8. Compute mean linear size using the relation $\overline{L} = I/P_L = 2/S_V$.

9. Label the I_{Seg} image. The maximum label value assigned to the region is the total number of grains in the microstructure image.
10. Compute the area of each region, which is size of each grain
11. Compute the average size of grains using area computed for each grain from Step 10.
12. Output the values of stereological parameters for quantitative analysis.

Algorithm 2: For processing two-component microstructure images

1. Input RGB microstructure image, I_{RGB}
2. Convert I_{RGB} image to grayscale image, I_{Gray}.
3. De-noise the image I_{Gray} using SMSF method and obtain filtered image, I_{Filt}.
4. Segment the I_{Filt} image using Otsu's segmentation method and obtain segmented binary image, I_{Seg}.
5. Generate grains boundary image, I_{Perim} of I_{Seg} image.
6. Compute volume fraction using the Eq.(1).
7. Compute P_L using Eq.(2).
8. Compute boundary (interface) density using relation; $S_v = 2P_L$.
9. Compute mean linear size using the relation $\overline{L} = I/P_L = 2/S_V$.
10. Compute mean linear distance using the relation $\overline{D} = (1-P_P)/P_L = 2(1-V_V)/S_V$
11. Label the I_{Seg} image. The maximum label value assigned to the region is the total number of grains in the microstructure image.
12. Compute the area of each region, which is size of each grain.
13. Compute the average size of grains using area computed for each grain from Step 12.
14. Output the values of stereological parameters for quantitative analysis.

The above algorithms are for one-component and two-component material microstructure image processing to determine most of the global stereological parameters.

4. EXPERIMENTAL RESULTS AND DISCUSSION

The experimentation has been performed on the experimental dataset of microstructure images (described in the Section 3.1) using Pentium Core 2 processor @ 3.2GHz with Matlab v7.9.

The Table 3 shows the results obtained by manual method and the Table 4 shows the results obtained by the proposed method corresponding to the one- and two-component microstructure images shown in the Fig. 4. The Table 5 presents the performance comparison between the manual and automated methods.

The Table 5 shows the absolute difference between the values of global stereological parameters obtained by the manual method and the proposed automated method corresponding to the sample microstructure images shown in the Fig. 4. The percentage error in average grain size (in µm) is found to vary in the range 5.5 to 9.1 in case of two-component materials, while it is varying in the range 1.8 to 5.3 in case of one-component materials. It is observed that the results obtained by the proposed method are close to the results obtained by the experts using manual method and these are within practical limits. The effort and time required for quantification of stereological parameters are minimized and accuracy is increased by using the proposed method based on digital image processing as compared to that for manual methods.

5. CONCLUSION

In this paper, a novel automated method for 3D quantitative analysis of microstructure images is presented. The proposed method adopts digital image processing techniques for quantification based on stereology. It works on a wide variety of materials of various compositions and different resolutions. The proposed method has potential to replace manual based quantification methods and provides more accurate results efficiently by saving effort, cost and time. The proposed method has practical importance in material quality test laboratories.

Table 3. Values of global stereological parameters derived by manual method, using the horizontal grid size with 5 probes each of size 300 µm on sample microstructure images each of size 470x365 µm (571x480 pixels) shown in Fig.4. (Scale factor: 1 pixel=0.625µm)

*Microstructure image in Fig 4.	V_v (%)	Tot. probe length (µm) (5 probes)	P_L= Counts/Tot. probe length counts	S_v=2*P_L	$\overline{L}$	$\overline{D}$	Avg. size of grains (µm)	Max. size of grains (µm)
(a)	0.140 (14%)	5*300µm = 1500µm	29/1500=0.0193	0.0386	7.2538	44.5596	110	11200
(b)	0.145 14.50%	1500µm	70/1500=0.0466	0.0932	3.1115	18.3476	90	3420
(c)	0.154 (15.40%)	1500µm	60/1500=0.0400	0.0800	3.8500	21.1500	92	16900
(d)	0.120 (12%)	1500µm	30/1500=0.0200	0.0400	6.0000	44.0000	130	2920
(e)	0.130 (13%)	1500µm	50/1500=0.0333	0.0666	3.9039	26.1261	260	1020
(j)	NA	1500µm	0.0215	0.0430	55.51	NA	9600	9915
(k)	NA	1500µm	0.0320	0.0640	31.25	NA	1200	19000
(l)	NA	1500µm	0.0410	0.0820	24.39	NA	1480	6200

*(a)-(e) Two-component and (j)-(l) One-component material microstructure images. NA-Not applicable

Table 4. Values of global stereological parameters obtained by proposed method on sample microstructure images of size 470x365 µm (571x480 pixels) shown in Fig.4. (Scale factor: 1 pixel=0.625µm)

*Microstructure image in Fig 4.	V_v	Tot. probe length (pixels)	P_L= Counts/Tot. probe length counts	$S_v=2*P_L$	$\overline{L}$	$\overline{D}$	Avg. size of grains in Pixels and µm	Max. size of grains in Pixels and µm
(a)	0.1389 13.89%	571*480 =274080	6620/274080 =0.0242	0.0484	5.7365	35.5560	161.40 Pixels 100.87µm	12012 Pixels 7507.50 µm
(b)	0.1305 13.05%	274080	11040/274080 =0.0403	0.0806	3.2385	21.5707	156.00 Pixels 97.50µm	3542 Pixels 2213.80µm
(c)	0.1483 14.83%	274080	10480/274080 =0.0382	0.0764	3.8824	22.2944	135.59Pixels 84.74µm	17004 Pixels 10628.00µm
(d)	0.1107 11.07%	274080	5250/274080 =0.0192	0.0384	5.7618	46.2457	190.60 Pixels 119.12µm	3012 Pixels 1882.50µm
(e)	0.1351 13.51%	274080	7910/274080 =0.0289	0.0577	4.6805	29.9534	394.02Pixels 246.2µm	1200 Pixels 750 µm
(j)	NA	274080	0.01485	0.0297	67.28	NA	4240 pixels 9813 µm	15701 pixels 9813 µm
(k)	NA	274080	0.02295	0.0459	43.35	NA	2353 pixels 1470.89 µm	30780 pixels 19237 µm
(l)	NA	274080	0.03675	0.0735	27.21	NA	2500 pixels 1562.50 µm	10250 pixels 6406 µm

*(a)-(e) Two-component and (j)-(l) One-component material microstructure images. NA-Not applicable

Table 5. Absolute difference between values of global stereological parameters obtained by the manual and automated methods for the sample microstructure images shown in the Fig.4.

Microstructure image in Fig 4.	V_v	P_L	S_v	$\overline{L}$	$\overline{D}$	Avg. size of grains in µm	Max. size of grains in µm
(a)	0.0010	0.0049	0.0098	1.5173	9.0036	09.13	188
(b)	0.0145	0.0063	0.0126	0.1270	3.2231	07.50	122
(c)	0.0057	0.0018	0.0036	0.0324	1.1444	07.26	104
(d)	0.0093	0.0008	0.0016	0.2382	2.2457	10.88	092
(e)	0.0051	0.0094	0.0244	0.7766	3.8272	13.74	180
(j)	NA	0.00665	0.0133	11.77	NA	213.00	97
(k)	NA	0.00905	0.0181	12.10	NA	270.00	237
(l)	NA	0.00425	0.0085	02.69	NA	82.00	206

6. REFERENCES

[1] ASM International Handbook Committee. 2004. ASM Hand book, Vol.9, Metallography and Microstructures. ASM International, USA.

[2] ASTM International. 2002. Standard Guide for Preparation of Metallographic Specimens, E3,Annual Book of ASTM Standards, Vol 3.01.

[3] ASTM International. 1999. Test Methods for Determining average grain size using semi automatic and automatic Image Analysis, E 1382-97,Annual Book ASTM Standards, Sec.3, pp 867-890.

[4] Russ J.C. 1999. Practical stereology, 2nd Edn., Plenum Press, New York.

[5] Underwood E.E. 1970. Quantitative Stereology, Addison-Wesley, USA.

[6] Wiebel. 1980. Stereological Methods, Vol. 1:Practical Methods for Biological Morphometry, Academic Press, New York.

[7] Deholf R.T. & Rhines. 1968. Quantitative microscopy, Mc. GrawHill, Newyork Otsu N. 1979.

[8] A Threshold level selection method from gray level histograms, IEEE Trans. Sys.Man., Cybernetics, Vol. 9, pp. 62-66.

[9] Exner H.E. 1996. Qualitative and Quantitative Surface Microscopy, Physical Metallography, Elsevier Science Publications, pp.993-1032.

[10] Ohser J and Mucklish. 2005. Statistical analysis of microstructure in material science, Wiley, Newyork.

[11] Howard C V and Reed M. 1998. Unbiased stereology, ISBN-387-91516-8, Springer.

[12] Pattan Prakash, Mytri V.D. and Hiremath P.S. 2009. Automatic Microstructure Image Analysis for Classification and Quantification of Phases of Material, in Proc. of Intl.Conf. on Systemics, Cybernetics and Informatics (ICSCI) Hyderabad, pp.308-311.

[13] Neil Brent and Russ J. C. 2012. Measuring shapes, CRC Press, Newyork.

[14] Exner H.E. 2004. Stereology and 3D Microscopy Useful alternatives or competitors in the quantitative Analysis of microstructures? Image Anal Stereol, vol 23, pp. 73-82.

[15]Microstructures Libraries: http://www.metalograf.de/start-eng.htm and www.doitpoms.ac.uk.

[16] P. S. Hiremath and Anita Sadashivappa. 2013. Selective Median Switching Filter for Noise Suppression in Microstructure Images of Material(SMSF), Intl' J. of Image Processing, Vol. 7:1, pp. 101-108.

[17] Pattan Prakash, Mytri V.D. and Hiremath P.S. 2011. Digital Microstructure Analysis System for Testing and Quantifying the Ductile Cast Iron, Intl' J. of Computer Applications (IJCA), Vol. 19, No.3, pp. 22-27.